

PAPER • OPEN ACCESS

Hexaferrite multiferroics: from bulk to thick films

To cite this article: T Koutzarova *et al* 2018 *J. Phys.: Conf. Ser.* **992** 012058

View the [article online](#) for updates and enhancements.

Related content

- [Inhomogeneous magnetoelectric interaction in multiferroics and related new physical effects](#)
Anatolii K Zvezdin and Aleksandr P Pyatakov
- [Room-temperature magnetoelectric effects in multiferroic Y-type hexaferrites](#)
Yanfen Chang, Kun Zhai, Yisheng Chai et al.
- [Pellet plant energy simulator](#)
D Bordeasu, T Vasquez Pulido and C Nielsen

Hexaferrite multiferroics: from bulk to thick films

T Koutzarova^{1,3}, Ch Ghelev¹, P Peneva¹, B Georgieva¹, S Kolev¹, B Vertruyen² and R Closset²

¹E. Djakov Institute of Electronics, Bulgarian Academy of Sciences,
72 Tzarigradsko Chaussee, 1784 Sofia, Bulgaria

²LSIC, Chemistry Department B6, University of Liege,
Sart Tilman, B-4000 Liege, Belgium

E-mail: tanya@ie.bas.bg, tatyana_koutzarova@ie.bas.bg

Abstract. We report studies of the structural and microstructural properties of $\text{Sr}_3\text{Co}_2\text{Fe}_{24}\text{O}_{41}$ in bulk form and as thick films. The precursor powders for the bulk form were prepared following the sol-gel auto-combustion method. The prepared pellets were synthesized at 1200 °C to produce $\text{Sr}_3\text{Co}_2\text{Fe}_{24}\text{O}_{41}$. The XRD spectra of the bulks showed the characteristic peaks corresponding to the Z-type hexaferrite structure as a main phase and second phases of CoFe_2O_4 and $\text{Sr}_3\text{Fe}_2\text{O}_{7-x}$. The microstructure analysis of the cross-section of the bulk pellets revealed a hexagonal sheet structure. Large areas were observed of packages of hexagonal sheets where the separate hexagonal particles were ordered along the c axis. $\text{Sr}_3\text{Co}_2\text{Fe}_{24}\text{O}_{41}$ thick films were deposited from a suspension containing the $\text{Sr}_3\text{Co}_2\text{Fe}_{24}\text{O}_{41}$ powder. The microstructural analysis of the thick films showed that the particles had the perfect hexagonal shape typical for hexaferrites.

1. Introduction

Multiferroics are multifunctional materials where two or more of the primary ferroic properties (ferromagnetism, ferroelectricity, ferroelasticity, ferrotoroidicity) coexist [1]. Although the ferroelectric behavior and ferromagnetism are, in general, mutually exclusive, there exist a few specific materials where these characteristics are present simultaneously, namely, yttrium-iron garnets, borates, rare-earth ferrites and manganites with a perovskite structure. In all of them, one can observe a magnetoelectric (ME) effect, whereby the magnetic phase can be controlled by applying an external electric field and, vice versa, the electric phase behavior can be influenced by an external magnetic field. The magnetoelectric effect can be exploited in both novel and in well-known devices, e.g., four-stage logic memory devices, electrical-field-controlled spintronic devices, electrical and magnetic field sensors in biomedicine, electric power generators, electrical-field-controlled microwave components, such as filters and switches for wireless technologies at up to terahertz frequencies, the latter area being essentially unexplored, etc. [2-6]. The main requirement to the applications of the magnetoelectric multiferroic materials is that the magneto-electric coupling be both large and active at room temperature and the magnetic ordering temperature be high. For the first time, the existence of a significant ME effect in hexaferrites at room temperature was reported by Kitagawa et al. [7], namely,

³ To whom any correspondence should be addressed.



the Z-type hexaferrite $\text{Sr}_3\text{Co}_2\text{Fe}_{24}\text{O}_{41}$ exhibited a low-field (~ 10 mT) magnetoelectric effect at room temperature.

The Z-type hexaferrites have a very complex crystal structure, being a combination of M-type and Y-type hexaferrites [8]. The unit cell consists of 140 atoms, distributed in S, R and T-blocks, which results in a crystal cell with an especially long c length. The extremely large unit cell is one of the reasons leading to difficulties in preparing this type of hexaferrites. Another reason is the small difference in the temperatures of phase transitions from one type of hexaferrite to another, which additionally hampers the preparation of single-phase samples, so that secondary phases of W and U-hexaferrites [9] often remain in the end product. This is why one needs techniques different from solid-state reactions, such as those of wet chemistry, to obtain samples with homogeneous composition. We will describe below our studies on the microstructural properties of $\text{Sr}_3\text{Co}_2\text{Fe}_{24}\text{O}_{41}$ in bulk form or as powders prepared by sol-gel auto-combustion. Often, ferrite powders are used for depositing thick or thin films with the primary materials being suspensions or pastes containing hexaferrite particles. Regardless of the technique for preparation used, the films' properties depend largely on the microstructural characteristics of the primary bulk materials. Thus, the hexaferrite particles should be homogeneous in shape and size to guarantee their fine dispersion and, hence, the smoothness of the coating formed. We, therefore, focused our attention on studying the structural and microstructural characteristics of the $\text{Sr}_3\text{Co}_2\text{Fe}_{24}\text{O}_{41}$ powders and bulk materials prepared by us. We will also present microstructural characteristics of $\text{Sr}_3\text{Co}_2\text{Fe}_{24}\text{O}_{41}$ thick film deposited from a suspension.

2. Experimental

The $\text{Sr}_3\text{Co}_2\text{Fe}_{24}\text{O}_{41}$ powders were synthesized by citric-acid sol-gel auto-combustion. The corresponding metal nitrates were used as starting materials. A citric acid solution was slowly added to the mixed solution of nitrates as a chelator. The solution was slowly evaporated to form a gel. This gel was dehydrated at 120°C to obtain the strontium-cobalt-iron citrate precursor. During the dehydration process, the gel turned into a fluffy mass and was burnt in a self-propagating combustion manner. During auto-combustion, the burning gel volume expanded rapidly. The auto-combusted powder was annealed at 600°C for five hours. The precursor powder obtained was pressed into disk-shaped pellets and synthesized at 1200°C for seven hours and then quenched rapidly to room temperature.

The thick film was deposited from a suspension containing the $\text{Sr}_3\text{Co}_2\text{Fe}_{24}\text{O}_{41}$. To prepare the suspension, the bulk samples were crushed and milled in a ball mill with agate mortar. The suspension was made by dispersing hexaferrite particles into a polyvinyl alcohol solution. The prepared suspension was dropped on the Al_2O_3 substrate. The as-deposited sample was slowly dried and annealed at 1200°C for five hours.

The samples were characterized using X-ray diffraction analysis with Cu- K_α radiation. The microstructures of the samples were observed by scanning electron microscopy (Philips ESEM XL30 FEG).

3. Results and discussion

Unlike the preparation of pure $\text{BaFe}_{12}\text{O}_{19}$ (M-type hexaferrite) using the citrate precursor technique, the Z-type phase powder cannot be produced as easily due to the complexity of its structure, which imposes the need of progressive transformation through intermediate ferrites before achieving the final structure required. We present data from the XRD analysis at different stages of the synthesis process. Figure 1 shows XRD spectra of powders after the sol-gel auto-combustion, of the powder synthesized at 600°C , and of a bulk sample annealed at 1200°C . The XRD spectra of the powder prepared by sol-gel auto-combustion show that the samples are amorphous, with only some low-intensity peaks of the CoFe_2O_4 spinel ferrite detected. Their intensity rises after the heat treatment at 600°C due to the higher crystallization degree of this spinel phase and the growth of the particles' size (figure 1 b). The XRD analysis of the bulk sample show the characteristic peaks corresponding to the $\text{Sr}_3\text{Co}_2\text{Fe}_{24}\text{O}_{41}$ as a main phase; second phases of not-reacted CoFe_2O_4 and $\text{Sr}_3\text{Fe}_2\text{O}_{7-x}$ were also observed. It is well known that the synthesis of Z-type hexaferrites produces other hexaferrites as well. For example, an M-type hexaferrite phase is formed due to the recrystallization process during cooling. To prevent the

appearance of an M-type phase in the samples, the pellets was rapidly quenched to room temperature. Thus, we found no traces of other hexaferrite phases after the $\text{Sr}_3\text{Co}_2\text{Fe}_{24}\text{O}_{41}$ synthesis.

Scanning electron microscopy was used to examine the morphology of the samples. Figure 2(a) shows a SEM image of the sample immediately after the completion of the auto-combustion process.

As seen, the material is amorphous. A typical porous structure is observed formed during the burn process. Some small agglomerated crystalline particles of CoFe_2O_4 can also be seen. After heat treatment at 600°C , the amount of crystalline CoFe_2O_4 auto-combusted powder increases. The particles are with a

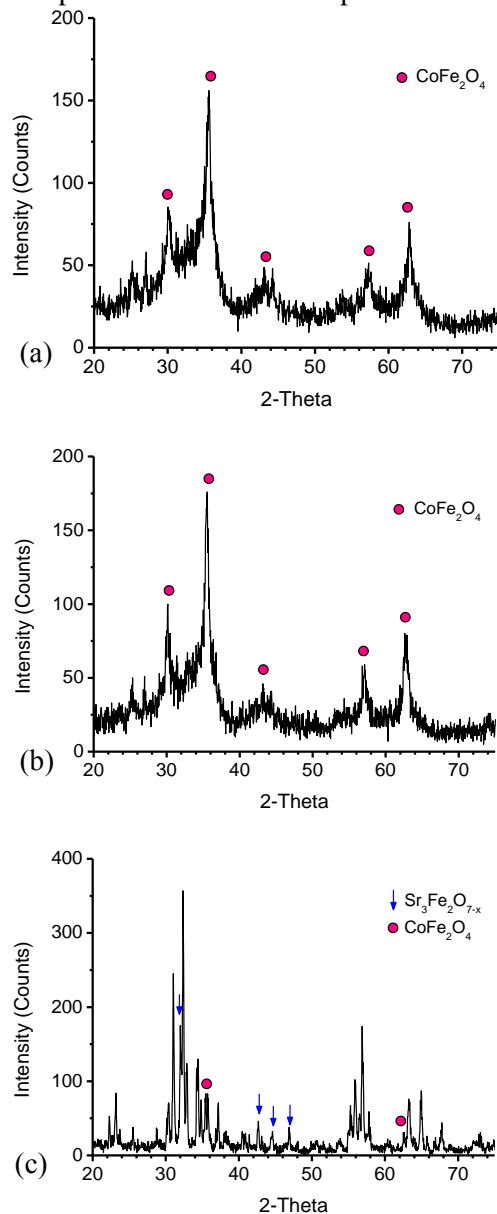


Figure 1. XRD spectra of $\text{Sr}_3\text{Co}_2\text{Fe}_{24}\text{O}_{41}$ (a) powder after auto-combustion, (b) powder annealed at 600°C , and (c) cross-section of a pellet.

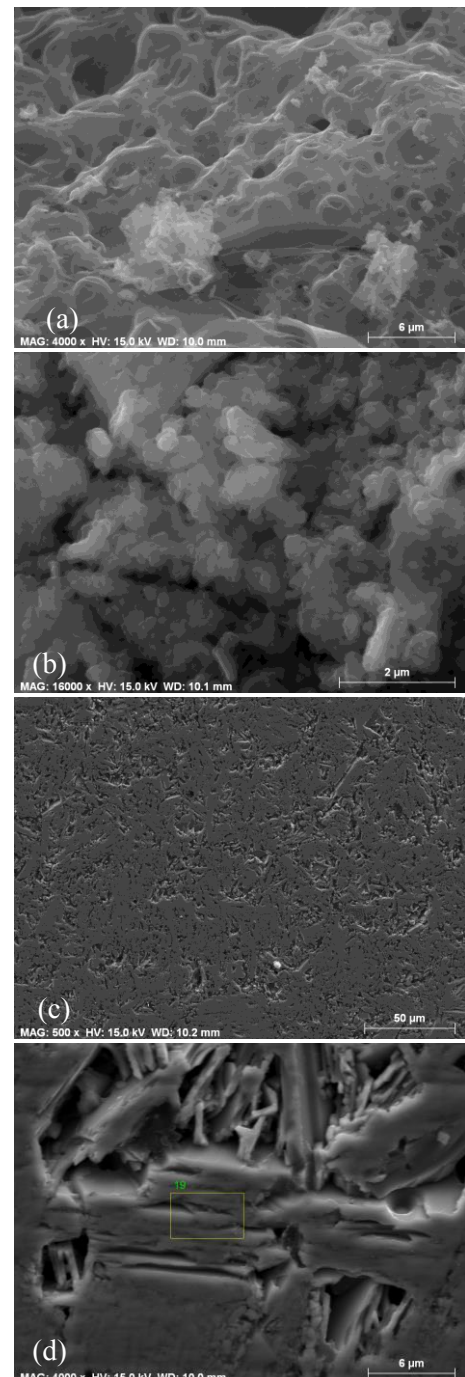


Figure 2. SEM images of $\text{Sr}_3\text{Co}_2\text{Fe}_{24}\text{O}_{41}$ (a) powder after auto-combustion, (b) powder annealed at 600°C , and (c, d) cross-section of a pellet.

spherical shape and very homogeneous in size (average particle size of 120 nm, figure 2b). The microstructure studies of the bulk pellets' cross-section show a hexagonal sheet structure (figure 2c, d). Large areas are observed of packages of hexagonal sheets where the separate hexagonal particles were ordered along the c axis. The difference in these areas' direction of formation has caused the appearance of pores in the pellet volume. The energy-dispersive X-ray analysis (EDX) data of these areas (area 19 on figure 2d) are presented in table 1. It indicates that the pellets are composed of Sr:Co:Fe in a ratio close to the stoichiometric one in $\text{Sr}_3\text{Co}_2\text{Fe}_{24}\text{O}_{41}$.

Figure 3 presents SEM images of a $\text{Sr}_3\text{Co}_2\text{Fe}_{24}\text{O}_{41}$ thick film. The microstructural analysis of the thick films prepared show a considerable roughness and porosity of their surface. Also, particles can be seen having the perfect hexagonal shape typical for hexaferrites.

Table 1. EDX analysis data of area 19 on figure 2d.

Element	Series	Norm. at. (%)	Stoichiometric ratio
oxygen	K-series	23.65	30.9
iron	K-series	14.86	25.0
cobalt	K-series	1.18	2.0
strontium	L-series	1.91	3.2

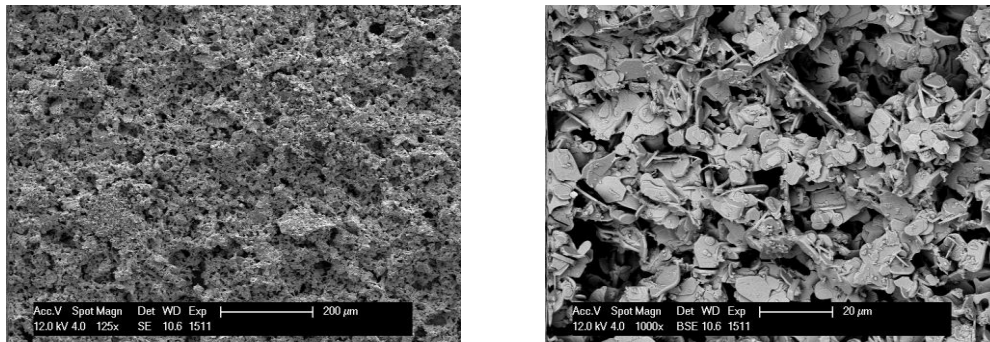


Figure 3. SEM images of $\text{Sr}_3\text{Co}_2\text{Fe}_{24}\text{O}_{41}$ thick films.

4. Conclusions

$\text{Sr}_3\text{Co}_2\text{Fe}_{24}\text{O}_{41}$ was synthesized by means of the auto-combustion method. Second phases of CoFe_2O_4 and $\text{Sr}_3\text{Fe}_2\text{O}_{7-x}$ were also observed. In contrast with the other techniques of Z-type hexaferrites preparation, no other hexaferrite phases were detected. Without applying an external magnetic field during pressing, the bulk samples exhibited large areas of texturing. The bulk samples were denser, which makes them suitable for use as targets in sputtering and pulsed laser deposition (PLD) of thin films. The thick films obtained by deposition from a suspension containing the $\text{Sr}_3\text{Co}_2\text{Fe}_{24}\text{O}_{41}$ particles were rough.

Acknowledgments

The work was supported by the Bulgarian National Science Fund under contract DN 08/4 “Novel functional ferrites-based magneto-electric structures” and a joint research project between Bulgarian Academy of Sciences and WBI, Belgium.

References

- [1] Schmid H 2004 *Magnetoelectric Interaction Phenomena in Crystals* eds Fiebig M, Eremenko and Vand Chupis I E (Dordrecht: Kluwer) p 35
- [2] Ebnabbasi K, Chen Y, Geiler A, Harris V and Vittoria C 2012 *J. Appl. Phys.* **111** 07C719.
- [3] Martin L W 2010 *Dalton Trans.* **39** 10813
- [4] Petrov R V, Murthy D V B, Sreenivasulu G and Srinivasan G 2013 *Microwave Opt. Technol. Lett.* **55** 533

- [5] Rao C N R, Sundaresan A and Saha R 2012 *J. Phys. Chem. Lett.* **3** 2237–46
- [6] Scott J F 2007 *Nat. Mater.* **6** 256
- [7] Kitagawa Y, Hiraoka Y, Honda T, Ishikura T, Nakamura H and Kimura T 2010 *Nat. Mater.* **9** 797
- [8] Mu Ch, Song Y, Wang L and Zhang H 2011 *J. Appl. Phys.* **109** 123925
- [9] Raju N, Shravan Kumar Reddy S, Ramesh J, Gopal Reddy Ch, Yadagiri Reddy P, Rama Reddy K, Sathe V G and Raghavendra Reddy V 2016 *J. Appl. Phys.* **120** 054103